Use of Vision Sensors and Lane Maps to Aid GPS/INS under a Limited GPS Satellite Constellation

John W. Allen, Auburn University
David M. Bevly, Auburn University

BIOGRAPHY

John was born in Demopolis, AL and grew up in Birmingham, Alabama. In 2007, he obtained his bachelor's degree in Mechanical Engineering from Auburn University. Currently, John is working on his master's degree and works in the GPS and Vehicle Dynamics Lab. John's research interest includes multi-sensor fusion for vehicle navigation, and modern control theory for ground vehicles.

David M. Bevly received his B.S. from Texas A&M University in 1995, M.S. from Massachusetts Institute of Technology in 1997, and Ph.D. from Stanford University in 2001 in mechanical engineering. He joined the faculty of the Department of Mechanical Engineering at Auburn University in 2001 as an assistant professor. Dr. Bevly's research interests include control systems, sensor fusion, GPS, state estimation, and parameter identification. His research focuses on vehicle dynamics as well as modeling and control of vehicle systems. Additionally, Dr. Bevly has developed algorithms for navigation and control of off-road vehicles and methods for identifying critical vehicle parameters using GPS and inertial sensors.

ABSTRACT

One major issue in implementation of a GPS/INS navigation system is the decrease in positioning performance in urban canyons. An urban canyon is any location where GPS satellite signals are blocked or corrupted by tall buildings. Tall buildings surrounding a GPS antenna will cause a masking affect on the antenna. Satellites that are at a low elevation angle will be blocked by buildings. Many of the signals that actually arrive at the antenna are corrupted by delays caused by multipath. A closely coupled GPS/INS navigation system with fault detection and exclusion can be used to combat the issue of multipath in urban areas. This paper will present a method of using vision measurements and a lane map to constrain the navigation system and thus improve observability.

Many modern GPS/INS navigation systems use a closely coupled architecture. A closely coupled navigation systems refers to a navigation systems that uses the pseudorange and pseudorange-rate measurements provided by a GPS receiver. A loosely coupled navigation system refers to a system that uses only the position and velocity reported by the GPS receiver. One advantage of a closely coupled architecture is its ability to provide limited IMU corrections while receiving measurements from less than four satellites. A loosely coupled architecture will provide no IMU corrections if the GPS receiver fails to track four or more satellites. Another advantage of the closely coupled system is the ability for the system designer to incorporate intelligent measurement rejection to reject bad pseudoranges and pseudorange-rates.

A closely coupled GPS/INS system with fault detection and measurement rejection can be used in an urban environment to mitigate navigation errors. The fault detection and measurement rejection will insure that bad pseudoranges and pseudorange-rates will not be used to compute the navigation solution. Furthermore, a complex elevation mask can be used to reject measurements from satellites that are believed to be currently blocked by buildings.

One issue with pseudorange measurement rejection is the possibility of loss of observability. If the number satellite measurements used falls under four, then the GPS/INS system will not be fully observable. Also, when using a limited number of satellite observations, the observability of the GPS/INS system is heavily affected by the geometry of the satellites used.

This paper proposes a method to increase observability of a GPS/INS system operating under limited satellite coverage. Extra range measurements from vision sensors

are used to supplement the GPS's pseudorange and pseudorange-rate measurements. Both LiDAR and camera measurements are used to measure a vehicle's lateral position in its current lane. The vision measurements provide local based positioning based of the lane. A map of the lane is used to relate the vision's local positioning and the GPS's global positioning. Also, constraining the navigation system's height above the lane map is used to further aid observability.

In order to test the performance of the navigation filter, real data from the NCAT test track in Opelika, Alabama will be used. The NCAT track has plenty of open sky; therefore, the solution using a full constellation of GPS satellites can be compared to the solution using only two GPS observations.

INTRODUCTION

In order to reduce the number of traffic fatalities that occur due to unintentional lane departures, many vehicle manufacturers are developing lane departure warning (LDW) systems. LDW systems alert the driver before the vehicle departs the lane. Most of the LDW systems in production now are solely based off camera measurements. A LDW camera uses feature extraction to determine lateral position in current lane. The feature used for a camera-based LDW system is the painted lane lines. A camera can not provide three-dimensional ranging information due to the unresolved distance from the camera to the feature of interest; though the camera can provide lateral position in a lane without resolving this distance. Camera-based LDW systems are prone to failures due to road, weather, and lighting conditions. A more in-depth look at how the camera is used to determine lane position can be found in [9].

Current research is underway to provide robustness to current camera-based LDW system by adding other types of sensors. A LiDAR (Light Detection And Ranging) is a active type of vision sensor. A LiDAR works like sonar. Instead of using sound waves, a LiDAR uses light ways to provide ranging. Unlike the camera, a LiDAR can provide three-dimensional ranging information. One drawback to the LiDAR is feature extraction can be more difficult than feature extraction using a camera. To overcome this, the LiDAR also provides reflectivity data. For the LDW case, a painted lane marker has a different reflectivity than the asphalt around it. The reflectivity data can be used to extract lane markers, and the ranging information can be used to provide an estimate of a vehicle's lateral position in the lane. A more in-depth look at how the LiDAR is used to determine lane position can be found in [2].

A camera and a LiDAR can both be used to estimate position in one-dimension in a three-dimensional space. GPS is used to estimate position and velocity in a four-dimensional space; the fourth dimension being time. This is why four GPS observations are needed to maintain observability of GNSS (Global Navigation Satellite System). GNSS is typically based off a global (ECEF) coordinate frame, while the camera and LiDAR work in a local (road) coordinate frame. This paper shows how to use a way-point based map to map satellite positions in the ECEF coordinate frame to a local coordinate frame based off the waypoint map. Doing this, a GNSS based off a local coordinate frame can be designed. The vision measurements can be used to resolve position in one axis of the local coordinate frame. Assuming a ground vehicle doesn't change height in the local coordinate frame, position resolution in the vertical axis can be resolved. This leaves the GNSS with one unresolved axis and an unresolved clock bias; therefore the GNSS proposed in the paper maintains full observability while only using two GPS observations. This could provide useful in urban navigation, or in any area where GPS observations are limited.

LANE MAP

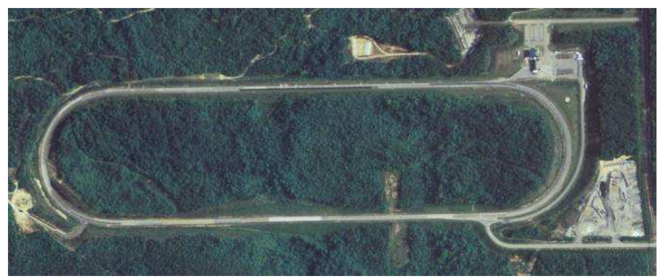

Figure 1. Top Down View of NCAT Track

All the data used for this paper was collected at the NCAT (National Center for Asphalt Technology) test track in Opelika, Alabama (Figure 1). The track is a two lane 1.8 mile oval with flat straights and 8° of bank in the corners. The track is used to test wear cause by large trucks on interstate asphalt.

A simple waypoint based map is used for this system. The map is necessary to relate global measurements (GPS) and local measurements (vision). Each waypoint's position is defined in the ECEF coordinate frame. The waypoint is assumed to reside in the center of the lane at ground level. This type of map works well for straight segments of road. Defining a curved road by waypoints is essentially a discretization of the curve. The closer the waypoints are together in a curve, the more accurate the map will be. The map used has two long straights and two 180 degree curves. The straights are defined by a line based off a waypoint at the start and end of the straight. The curves are based off several waypoints that are spaced approximately 10 meters apart.

The proposed method of sensor fusion for lane positioning requires a detailed map of the lane in which the vehicle is traveling. This is one limiting factor in the implementation of the proposed method. Current GPS receivers for personal vehicle navigation have a map database; however, in order to ensure accuracy, the map data base for this algorithm needs to be precise. GPS with RTK corrections can provide accuracy on the centimeter level; but surveying using GPS can be time-consuming. Surveying lanes will also require the road to be free of traffic. Future developments of lane positioning methods could be used to back out lane position relative to a known vehicle location. Such systems would need to be based off differential GPS measurements and precise attitude determination.

In order to get a detailed map of the NCAT test track, the outside lane of the track was surveyed. The survey was conducted with two Novatel GPS receivers. Both of the receivers provide a narrow integer solution with corrections from an on-site base station. A more detailed explanation of how the survey was conducted can be found in [1].

NAVIGATION FILTER

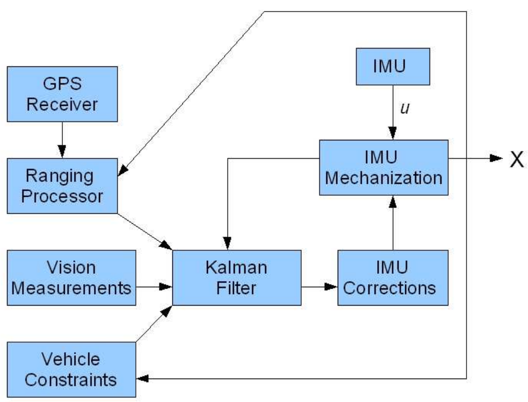

Figure 2. Filter Architecture

A Kalman Filter [5] is the core of the proposed lane tracking estimation algorithm. An Extended Kalman Filter is used because both the time update and the measurement update are constructed using non-linear equations. Figure 2 shows the architecture of the navigation filter. Many traditional navigation filters use the ECEF or tangential plane coordinate frames for navigation. The base navigation coordinate frame for this project is a modification of the tangential plane. The orientation of the plane is based off the track map. The navigation frame is also called the road frame. The road frame is a coordinate frame that is attached to the road. The position and velocity states of the filter are expressed in the road frame. The heading state (Ψ) is measured from the x-axis of the road frame; therefore, this heading state is essentially the heading in the lane.

$$X = \begin{bmatrix} x \\ y \\ z \\ \dot{x} \\ \dot{y} \\ \dot{z} \\ b_{ax} \\ b_{ay} \\ b_{az} \\ \psi \\ b_{\psi} \\ ct_u \\ c\dot{t}_u \end{bmatrix} = \begin{bmatrix} x_1 \\ x_2 \\ x \\ x_4 \\ x_5 \\ x_6 \\ x_7 \\ x_8 \\ x_9 \\ x_{10} \\ x_{11} \\ x_{12} \\ x_{13} \end{bmatrix} \quad (1) \qquad u = \begin{bmatrix} \ddot{x} + b_{ax} \\ \ddot{y} + b_{ay} \\ \ddot{z} + b_{az} \\ \dot{\psi} + b_{\Psi} \end{bmatrix} = \begin{bmatrix} u_1 \\ u_2 \\ u_3 \\ u_4 \end{bmatrix} \quad (2)$$

The navigation filter is a four degree of freedom filter. The vehicle is assumed to neither pitch nor roll with respect to the road frame. Equation 1 shows the state vector. It consist of three position states, three velocity states, three accelerometer bias states, one attitude state (road heading), one gyro bias state, a clock bias state, and a clock drift state. The input to the system is shown in equation 2. The input comes from the IMU's measurements. The measurements from the IMU are considered to be biased, and the bias is estimated by the navigation filter.

NAVIGATION COORDINATE FRAME

The navigation coordinate frame used is based off a waypoint map. The navigation coordinate frame is a NED (North, East, Down) coordinate frame that is oriented in such a way that the x-axis of the coordinate frame points from the last waypoint passed (base waypoint) to the next waypoint the vehicle will pass. The z-axis of the coordinate frame points down, and the y-axis of the coordinate frame points to the right in reference to the road when facing the direction of travel. A rotation matrix is needed to map satellite positions and velocities from the ECEF coordinate frame to the navigation coordinate frame. In order to construct the rotation matrix the longitude and latitude of the base waypoint must be known. Also, the pitch and heading of the coordinate frame with respect to the North, East, Down coordinate frame must be known.

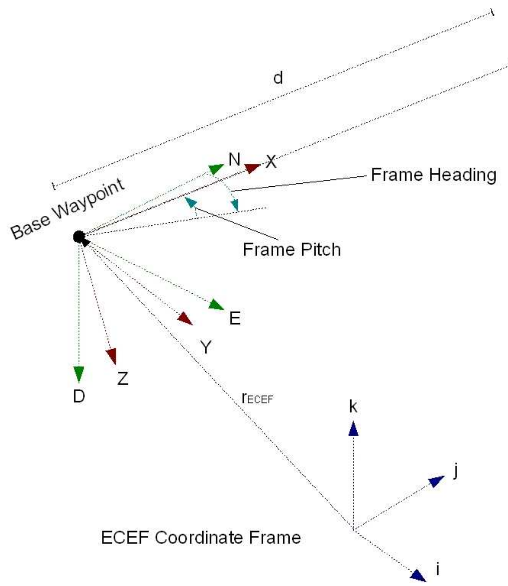

Figure 3. Navigation Coordinate Frame

Figure 3 is a drawing of the navigation coordinate frame. The lane survey provides the position of the waypoints in the ECEF coordinate frame. The longitude and latitude of the waypoints can be solved post-survey using an iterative process. The algorithm used to solve for longitude and latitude can be found in [6]. Equation 3 shows the rotation matrix from the ECEF coordinate frame to the NED coordinate frame.

$$C_{ECEF}^{NED} = \begin{bmatrix} -\sin(\phi)\cos(\lambda) & -\sin(\phi)\sin(\lambda) & \cos(\phi) \\ -\sin(\lambda) & \cos(\lambda) & 0 \\ -\cos(\phi)\cos(\lambda) & -\cos(\phi)\sin(\lambda) & -\sin(\phi) \end{bmatrix} \tag{3}$$

λ - Longitude of frame origin

ϕ - Latitude of frame origin

P_o - Position of frame origin in ECEF

$$P_{NED} = C_{ECEF}^{NED}(P_{ECEF} - P_o) \tag{4}$$

Position measured in the ECEF coordinate frame can be mapped to the NED frame using equation 4 [6]. P_o is the position of the origin of the NED coordinate frame expressed in ECEF coordinates (P_o = [x ,y,z]^T). P_{ECEF} is the position of the point of interest in ECEF coordinates; P_{NED} is the position of the point of interest in NED coordinates.

The heading and pitch of the navigation coordinate frame can be solved using equation 4 and some simple geometry. P_o in this case is the position of the base waypoint. P_{ECEF} is the position of the next waypoint the vehicle will pass in the ECEF coordinate frame. P_{NED} will be the position of the next waypoint expressed in the NED coordinate frame. The heading and pitch of the navigation coordinate frame must be known in order to construct the rotation matrix from the NED coordinate frame to the navigation coordinate frame (7) [7]. The heading of the coordinate frame is in between +/- 180 degrees. The navigation coordinate frame's heading can be solved using equation 5. The pitch, or grade, of the coordinate frame is in between +/- 90 degrees. The navigation coordinate frame's pitch can be solved using equation 6. The navigation coordinate frame is assumed to have zero roll in relation to the NED coordinate frame.

$$\theta_1 = a\tan 2(p_{NED,2}, p_{NED,1}) \tag{5}$$

$$\theta_2 = a\tan(-p_{NED,3} / (p_{NED,1}{}^2 + p_{NED,2}{}^2)^{1/2}) \tag{6}$$

$$C_{NED}^{NAV} = \begin{bmatrix} \cos(\theta_1)\cos(\theta_2) & \sin(\theta_1)\cos(\theta_2) & -\sin(\theta_2) \\ -\sin(\theta_1) & \cos(\theta_1) & 0 \\ \cos(\theta_1)\sin(\theta_2) & \sin(\theta_1)\sin(\theta_2) & \cos(\theta_2) \end{bmatrix} \tag{7}$$

Multiplying the rotation matrix from the NED coordinate frame to the navigation coordinate frame and the rotation matrix from the ECEF coordinate frame to the NED coordinate frame will result in a matrix that maps ECEF coordinates to navigation frame coordinates (8). Equation 9 is used to map the GPS satellite positions from the ECEF coordinate frame to the navigation coordinate frame. Equation 10 is used to map the GPS satellite velocities from the ECEF coordinate frame to the navigation coordinate frame.

$$C_{ECEF}^{NAV} = C_{NED}^{NAV} * C_{ECEF}^{NED} \tag{8}$$

$$P_{NAV} = C_{ECEF}^{NAV}(P_{ECEF} - P_o) \tag{9}$$

$$V_{NAV} = C_{ECEF}^{NAV}(V_{ECEF}) \tag{10}$$

$$d = \sqrt{p_{NED,1}{}^2 + p_{NED,2}{}^2 + p_{NED,3}{}^2} \tag{11}$$

Equation 11 shows how to solve for the distance between waypoints (d). P_{NED} is the position of the next waypoint the vehicle will pass in the NED coordinate frame. In order to use a coordinate frame based off a waypoint map the position of each waypoint in the ECEF coordinate frame, the longitude and latitude of each waypoint, the heading and pitch of each segment, and the distance of each segment must be know. This information can be saved in a map database for use in by the navigation filter.

IMU MECHANIZATION

The measurements from the IMU can be used to propagate the filter's states between GPS, camera, and LiDAR measurements. Equation 12 shows the equations of motion used to propagate the states. The equations of motion for this system are very simple due to the choice of navigation coordinate frame. The vector g is the gravity vector expressed in the navigation coordinate frame. The gravity vector can be approximated by multiplying the NED to NAV rotation matrix by $[0,0,9.81]^T$. The IMU inputs (u) are used in conjunction with Runge Kutta 4th order integration to propagate the states.

$$\dot{X} = f(X,u) = \begin{bmatrix} x_4 \\ x_5 \\ x_6 \\ (u_1 - x_7)\cos(x_{10}) - (u_2 - x_8)\sin(x_{10}) + g_1 \\ (u_1 - x_7)\sin(x_{10}) + (u_2 - x_8)\cos(x_{10}) + g_2 \\ u_3 - x_9 + g_3 \\ 0 \\ 0 \\ 0 \\ u_4 - x_{11} \\ 0 \\ x_{12} \\ 0 \end{bmatrix} \tag{12}$$

Equation 13 is used to update the state covariance matrix at each time update. The IMU measurements come in at a discrete time; so equation 13 represents a discrete update of the state covariance matrix. The matrix A is obtained by taking the partial derivative of each equation of motion with respect to each state (14). The discrete version of A can be obtained using equation 15.

$$P = A_D P A_D^T + (BQB^T)dt \tag{13}$$

$$a_{[i,j]} = \frac{\partial f_{[i]}}{\partial x_{[j]}}(\hat{x},u) \tag{14}$$

$$A_D = e^{A*dt} \tag{15}$$

The B matrix is obtained by taking the partial derivative of each equation of motion with respect to each noise source (17). Equation 16 shows the equations of motion with the noise sources add in (ν_i). There are nine different noise sources. Four noise sources (ν_1- ν_4) are from the IMU inputs. Five noise sources (ν_5- ν_9) are necessary to allow estimation of IMU biases and clock drift. Q is the process noise covariance matrix. The size of Q is defined by the number of noise sources (9x9). Q is a constant diagonal matrix. The first four values on the diagonal of Q are defined as the variance of each IMU input. The last five values on the diagonal of Q are tuned to give desired bias and clock drift estimation characteristics.

$$\dot{X} = f(X,u) = \begin{bmatrix} x_4 \\ x_5 \\ x_6 \\ (u_1 - x_7 + \nu_1)\cos(x_{10}) - (u_2 - x_8 + \nu_2)\sin(x_{10}) + g_1 \\ (u_1 - x_7 + \nu_1)\sin(x_{10}) + (u_2 - x_8 + \nu_2)\cos(x_{10}) + g_2 \\ u_3 - x_9 + g_3 + \nu_3 \\ \nu_5 \\ \nu_6 \\ \nu_7 \\ u_4 - x_{11} + \nu_4 \\ \nu_8 \\ x_{12} \\ \nu_9 \end{bmatrix} \tag{16}$$

$$b_{[i,j]} = \frac{\partial f_{[i]}}{\partial \nu_{[j]}}(\hat{x},u) \tag{17}$$

MEASUREMENT UPDATE

Equations 18-20 are used to update the state vector and the state noise covariance matrix after a measurement is received [8]. K is the Kalman gain matrix. R is the measurement noise covariance matrix. R is a diagonal matrix that is mxm where m is the number of measurements. The diagonal element $r_{i,i}$ is equal to the variance of measurement i. Z is the measurement residual vector. The residual vector is equal to the difference in the measurement and the estimated measurement.

$$K = PH^T(HPH^T + R) \tag{18}$$

$$\hat{x} = \hat{x} + KZ \tag{19}$$

$$P = (I - KH)P \tag{20}$$

The H matrix varies depending on what type of measurement is being used. Equation 21 shows a traditional H matrix for a closely coupled GPS measurement update with four satellite observations. Each observation is represented by two rows in the H matrix. The first row represents a pseudorange measurement, and the second row represents a pseudorange rate measurement. Four independent satellite observations are need for the navigation filter to be fully observable. If more than four observations are available, the H matrix can be modified by adding two rows for each additional observation. If less than four observations are available, then the navigation filter will not be fully observable; however, a measurement update can take place using the observations available.

$$H = \begin{bmatrix} a_1 & b_1 & c_1 & 0 & 0 & 0 & 0 & 0 & 0 & 0 & 0 & -1 & 0 \\ 0 & 0 & 0 & a_1 & b_1 & c_1 & 0 & 0 & 0 & 0 & 0 & 0 & -1 \\ a_2 & b_2 & c_2 & 0 & 0 & 0 & 0 & 0 & 0 & 0 & 0 & -1 & 0 \\ 0 & 0 & 0 & a_2 & b_2 & c_2 & 0 & 0 & 0 & 0 & 0 & 0 & -1 \\ a_3 & b_3 & c_3 & 0 & 0 & 0 & 0 & 0 & 0 & 0 & 0 & -1 & 0 \\ 0 & 0 & 0 & a_3 & b_3 & c_3 & 0 & 0 & 0 & 0 & 0 & 0 & -1 \\ a_4 & b_4 & c_4 & 0 & 0 & 0 & 0 & 0 & 0 & 0 & 0 & -1 & 0 \\ 0 & 0 & 0 & a_4 & b_4 & c_4 & 0 & 0 & 0 & 0 & 0 & 0 & -1 \\ 0 & 0 & 0 & 0 & 0 & 0 & 0 & 0 & 0 & 1 & 0 & 0 & 0 \end{bmatrix} \quad (21)$$

A measurement of the heading angle is also need for the navigation filter to be fully observable. The last row of the H matrix represents a measurement of the heading angle. This measurement is obtained by assuming the vehicle has no sideslip; therefore, the heading angle is equal to the course of the vehicle (22). This measurement is only used if the vehicle's absolute velocity is above some minimum value.

$$\upsilon = a\tan(\hat{x}_2 / \hat{x}_1) \quad (22)$$

The vector $[a_i,b_i,c_i]$ represents a unit vector pointing from the user to the GPS satellite from which observation i originated. This unit vector is expressed in the navigation coordinate frame. In order to find this unit vector, the positions and velocities provided by the GPS ephemeris must be rotated into the navigation coordinate frame. This can be done using equations 9 and 10. The heading and elevation angles can be solved using equations 5 and 6 where $P_{NED}=[a_i,b_i,c_i]$. The heading angle is in between +/- 180 degrees. A zero degree satellite heading angle would represent a satellite that is directly in front of the traveling vehicle. A 180 degree satellite heading angle would represent a satellite that is directly behind the traveling vehicle.

The H matrix can be modified to incorporate vision measurements and vehicle constrains. Equation 23 shows the modified H matrix with two GPS observations. The first four rows of the H matrix represent the two GPS observations. The fifth row represents the vision measurement. Since the navigation coordinate frame is based off the lane map, the LiDAR and camera are assumed to give a direct measurement of the lateral position state. The sixth and seventh rows represent a vehicle constraint. Since the navigation coordinate frame is based off the lane map, the vertical position state can be assumed to be fixed. The measurement value for this state is simply the height of the IMU off the ground. If the vertical position is fixed, then the vertical velocity is equal to zero. The last row represents the measurement of the vehicles heading in the lane.

$$H = \begin{bmatrix} a_1 & b_1 & c_1 & 0 & 0 & 0 & 0 & 0 & 0 & 0 & 0 & -1 & 0 \\ 0 & 0 & 0 & a_1 & b_1 & c_1 & 0 & 0 & 0 & 0 & 0 & 0 & -1 \\ a_2 & b_2 & c_2 & 0 & 0 & 0 & 0 & 0 & 0 & 0 & 0 & -1 & 0 \\ 0 & 0 & 0 & a_2 & b_2 & c_2 & 0 & 0 & 0 & 0 & 0 & 0 & -1 \\ 0 & 1 & 0 & 0 & 0 & 0 & 0 & 0 & 0 & 0 & 0 & 0 & 0 \\ 0 & 0 & 1 & 0 & 0 & 0 & 0 & 0 & 0 & 0 & 0 & 0 & 0 \\ 0 & 0 & 0 & 0 & 0 & 1 & 0 & 0 & 0 & 0 & 0 & 0 & 0 \\ 0 & 0 & 0 & 0 & 0 & 0 & 0 & 0 & 0 & 1 & 0 & 0 & 0 \end{bmatrix} \quad (23)$$

For the results shown, a fault detection and exclusion algorithm was used to reject bad GPS measurements. The algorithm works by monitoring the computed residuals. If a measurement's residual lies outside of a certain bound, the measurement is not used. The bound is based off the estimated standard deviation of that measurement. A more in depth look at the algorithm used can be found in [5]. It is worth noting that fault detection and exclusion has been proven to be more effective when using a high sensitivity GPS receiver like a Novatel ProPak. Also, based off this work, the fault detection is much more effective when using a full constellation of satellites. The results do show a slight improvement in performance when using a limited satellite constellation.

OBSERVABILTY ANYLSIS

The observability of the proposed navigation filter must be checked in order to see if the filter will work with only two GPS observations. The observability of the filter can be checked using the observability matrix defined by equation 24 [3]. If the rank of this matrix is full (rank=13), then the filter will be observable. The A matrix is obtained from equation 14. Since the equations of motion for the system are nonlinear, the A matrix will be a function of x_7, x_8, x_{10}, u_1, and u_2; however, changing these values has no effect on the observability of the system. If the H matrix in equation 21 is plugged into equation 24, then the rank of the observability matrix will be full. This is contingent on the fact that the unit vector to each of the different satellites is independent of one another.

$$OBS = \begin{bmatrix} C \\ CA \\ CA^2 \\ \cdots \\ CA^{13} \end{bmatrix} \quad (24)$$

In order to test the observability of the proposed navigation filter, the H matrix from equation 23 can be placed into equation 24. The observability will depend on the values chosen for the unit vectors to each of the satellites. Equation 25 shows an H matrix with two GPS observations. The satellite geometry is set up to represent a satellite in front and behind the vehicle. The elevation angle for each satellite is 45 degrees. If the H matrix from equation 25 is plugged into equation 24, then the observability matrix will be full rank. This means the navigation filter is fully observable.

$$H = \begin{bmatrix} .707 & 0 & -.707 & 0 & 0 & 0 & 0 & 0 & 0 & 0 & 0 & -1 & 0 \\ 0 & 0 & 0 & .707 & 0 & -.707 & 0 & 0 & 0 & 0 & 0 & 0 & -1 \\ -.707 & 0 & -.707 & 0 & 0 & 0 & 0 & 0 & 0 & 0 & 0 & -1 & 0 \\ 0 & 0 & 0 & -.707 & 0 & -.707 & 0 & 0 & 0 & 0 & 0 & 0 & -1 \\ 0 & 1 & 0 & 0 & 0 & 0 & 0 & 0 & 0 & 0 & 0 & 0 & 0 \\ 0 & 0 & 1 & 0 & 0 & 0 & 0 & 0 & 0 & 0 & 0 & 0 & 0 \\ 0 & 0 & 0 & 0 & 0 & 1 & 0 & 0 & 0 & 0 & 0 & 0 & 0 \\ 0 & 0 & 0 & 0 & 0 & 0 & 0 & 0 & 0 & 1 & 0 & 0 & 0 \end{bmatrix} \quad (25)$$

Equation 26 represents a satellite geometry where the GPS satellites lie at exactly plus and minus 90 degrees from the direction of travel. Both the satellites have an elevation angle of 45 degrees. If the H matrix from equation 26 is plugged into equation 24, then the observability matrix will not be full rank. This means the navigation filter is not fully observable.

$$H = \begin{bmatrix} 0 & .707 & -.707 & 0 & 0 & 0 & 0 & 0 & 0 & 0 & 0 & -1 & 0 \\ 0 & 0 & 0 & 0 & .707 & -.707 & 0 & 0 & 0 & 0 & 0 & 0 & -1 \\ 0 & -.707 & -.707 & 0 & 0 & 0 & 0 & 0 & 0 & 0 & 0 & -1 & 0 \\ 0 & 0 & 0 & 0 & -.707 & -.707 & 0 & 0 & 0 & 0 & 0 & 0 & -1 \\ 0 & 1 & 0 & 0 & 0 & 0 & 0 & 0 & 0 & 0 & 0 & 0 & 0 \\ 0 & 0 & 1 & 0 & 0 & 0 & 0 & 0 & 0 & 0 & 0 & 0 & 0 \\ 0 & 0 & 0 & 0 & 0 & 1 & 0 & 0 & 0 & 0 & 0 & 0 & 0 \\ 0 & 0 & 0 & 0 & 0 & 0 & 0 & 0 & 0 & 1 & 0 & 0 & 0 \end{bmatrix} \quad (26)$$

As it turns out, the only time the navigation filter is unobservable is when the satellites are exactly perpendicular to the direction of travel. Both satellites must be perpendicular. Even if one of the satellites is not exactly perpendicular to the direction of travel, then the filter will be observable. This can be visualized in equation 26. Both the first and fourth columns are stacked with zeros; therefore, the measurements provide no information on the longitudinal position and velocity states. Also, the elevation angles of the satellites have no effect on observability.

NAVIGATION COORDINATE FRAME UPDATES

Since the navigation frame is based off the global position of the vehicle, the longitudinal position of the vehicle in the road coordinate frame must be checked after every state update. If the longitudinal position exceeds the length of the current road frame, then the vehicle has passed into the next road coordinate frame. If the vehicle has passed into the next road coordinate frame then the estimates of the states are expressed in the old road coordinate frame; therefore the states must be mapped into the new road (navigation) coordinate frame. If the vehicle has passed into the next road coordinate frame, the first step to update the states is to form a rotation matrix based off of the change in coordinate frame heading and pitch (27).

$$\Delta\theta = \begin{bmatrix} \Delta\theta_1 \\ \Delta\theta_2 \end{bmatrix} = \begin{bmatrix} \theta_{1,i+1} - \theta_{1,i} \\ \theta_{2,i+1} - \theta_{2,i} \end{bmatrix}$$
$$\Delta C = \begin{bmatrix} \cos(\Delta\theta_1)\cos(\Delta\theta_2) & \sin(\Delta\theta_2) & -\sin(\Delta\theta_2) \\ -\sin(\Delta\theta_1) & \cos(\Delta\theta_1) & 0 \\ \cos(\Delta\theta_1)\sin(\Delta\theta_2) & \sin(\Delta\theta_1)\sin(\Delta\theta_2) & \cos(\Delta\theta_2) \end{bmatrix} \quad (27)$$

The heading state can be updated by subtracting $\Delta\theta_1$ from the current estimate of vehicle heading in the lane (28).

$$X_{10} = X_{10} - \Delta\theta_1 \quad (28)$$

The next step consists of updating the position state estimates. Equation 29 shows how to update the position states using the rotation matrix (27).

$$X_{1:3} = \Delta C\left(X_{1:3} - \begin{bmatrix} d_i \\ 0 \\ 0 \end{bmatrix}\right) \quad (29)$$

Equation 30 shows how to map the velocity states into the new road coordinate frame.

$$X_{4:6} = \Delta C(X_{4:6}) \quad (30)$$

After completing the above steps, the filter's state vector will be expressed in terms of the new road coordinate frame. This process must be performed every time the vehicle moves into a new road coordinate frame. Comparing the longitudinal position state (X_1) to d_i after every time and measurement update will ensure the navigation filter is operating in the appropriate coordinate frame. The state covariance matrix is not updated after a change in coordinate frame. The effect of not updating the state covariance matrix is negligible if the change in coordinate frame attitude is small.

EFFECTS OF CHANGES IN NAVIGATION COORDINATE FRAME PITCH

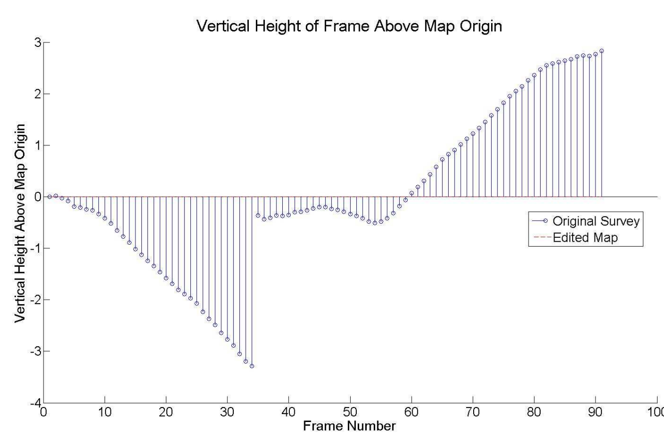

Figure 4. Height of Waypoints Above Initial Waypoint

One issue with using a waypoint map based coordinate frame is drastic changes in coordinate frame attitude can cause a spike in the estimate error. The effect worsens as vehicle speed increases. When using the lane map of the NCAT test track, no known issues arises due to drastic changes in coordinate frame heading; however, there has been a problem with drastic changes in pitch. Figure 4 shows the height above the initial waypoint for every waypoint that makes up the NCAT outside lane map. There are two drastic changes in height. These height changes cause four drastic changes in coordinate frame pitch.

These changes in height correspond to gaps in the survey. The survey took two days to complete. When the survey was picked up on the second day, there was a large jump in vertical position reported by the Novatel receiver using RTK corrections. GPS is known to be more inaccurate in the vertical axis due to poor satellite geometry. The survey ended where it started, and a large jump can also be seen when the lane map wraps around. It is important to note that the sharp changes in coordinate frame pitch where caused by GPS based surveying error.

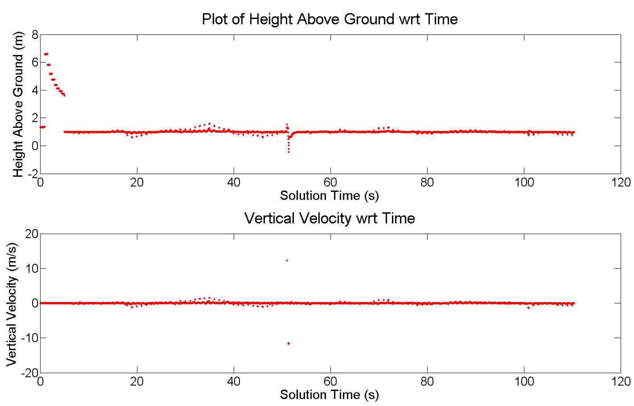

Figure 5. Filtered Vehicle Vertical Height and Velocity With Coordinate Frame Pitch Change

Figure 5 shows the vertical position and velocity reported by the navigation filter. For this example, the vehicle is traveling at 70 miles per hour around the test track. A full constellation of GPS satellites was used. The double pitch change due the single height change on the waypoint map can be seen by the two disturbances in vertical velocity at 50 seconds. The vehicle has a large velocity component in the x direction (longitudinal to the road) when it passes from one frame to the next. When the vehicle passes the large pitch changes in the map, a large portion of the longitudinal velocity is then rotated into the vertical axis. These disturbances in velocity propagate into the vertical position estimate. For the results provided, the vertical errors in the map where smoothed to combat the false pitch changes.

RESULTS

All the results shown in this paper comes from data collected at the NCAT test track. The equipment used includes a Novatel ProPak GPS receiver, Crossbow 440 IMU, IBEO ALASCA XT LiDAR, and a Logitech QuickCam Pro 9000. The data from these sensors was collected on a PC for post-processing. The data was post processed using C++; all plots were created with Matlab. The date run consist of one lap around the track. The vehicle speed is 70 miles per hour. The red dots represent the results of the navigation filter using all the available GPS observations. The blue dots represent the results of the navigation filter using only two GPS observations. The two observations come from satellites that are approximately parallel with the front and back straightaway of the test track.

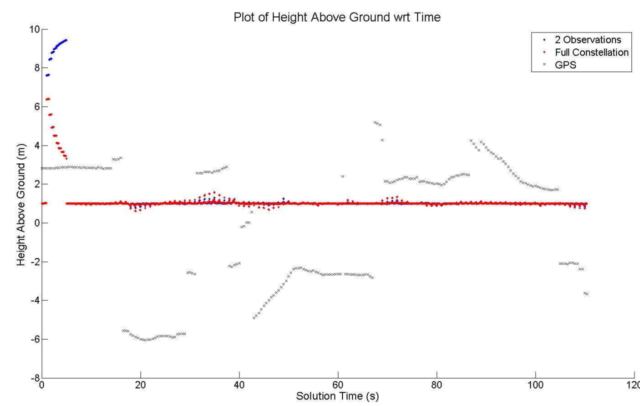

Figure 6. Estimated Vertical Position

The vertical position and velocity is shown in figure 6. The black x's correspond to the GPS's reported height above the navigation coordinate frame. Providing a measurement of the vehicles height above the map works well at constraining the vehicle's height above the map. A navigation filter using no height constraint would have a larger fluctuation in estimated vertical height.

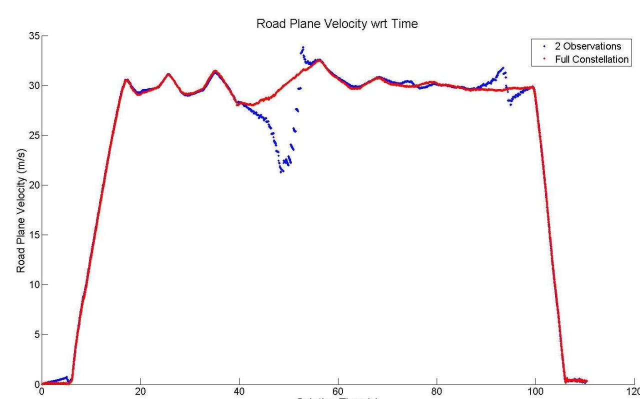

Figure 7. Planer Velocity Solution

Figure 7 shows the planer velocity estimated by the navigation filter. The planer velocity is simply the magnitude of the first two velocity states. The solution only using two observations has two distinct areas where the solution drifts off.

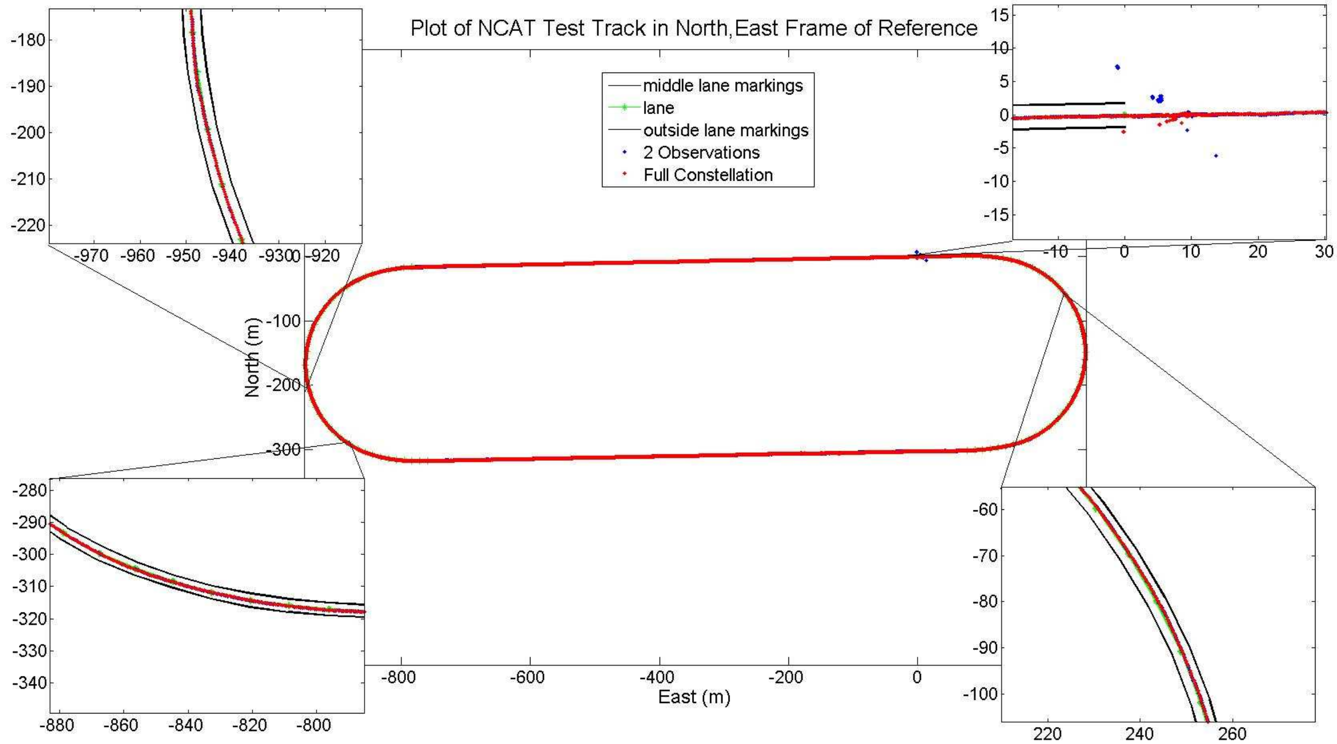

Figure 8. Planar Position Solution Using Two Sets of Observations

This is due to bad satellite geometry. The observability analysis says that the navigation filter is unobservable when the unit vectors to the two GPS satellites are perpendicular to the direction of travel. These unobservable sections can be thought of as asymptotes. The closer the unit vectors are to these asymptotes, the worse the estimation error will be.

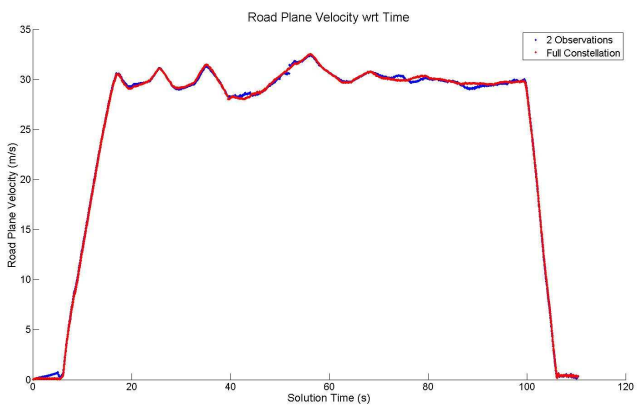

Figure 9. Planar Velocity Solution Using Two Sets of Observations

For the two observation solution, the unit vectors to the two GPS satellites are parallel with the direction of travel on the front and back straights; however, since the track is circular, there are two points in the turns where the filter approaches the unobservable asymptotes. At these points, there is a large spike in the planar velocity estimation error. In order to prove this is the cause of the error, figure 9 shows the planer velocity estimates using two different sets of GPS observations. While the vehicle is on the straights, the two observation solution uses the same satellites as before; however, while the vehicle is in the turns, another set of GPS observations is used that is more parallel with the direction of travel in the turns. Figure 8 shows the planer position estimates for the full constellation solution and the solution using two different pairs of GPS observations.

CONCLUSIONS

The observability analysis of a navigation filter using GPS/IMU, vision, and lane maps show that it is possible for the system to still be fully observable while only using two GPS observations. The observability analysis seems to be mush more forgiving than real life implementation. The observability analysis suggest that the navigation filter will work as long as the two GPS observations do not lie directly perpendicular to the direction of travel; however, the analysis of the real data suggest otherwise. The system only performs well when the two GPS observations are parallel with the direction of travel. Also, two observations should be in opposite directions. The observability analysis suggests the observations can come from the same direction. This is not the case for real implementation. The observations must be close to parallel with the direction of travel; and, the observations must have close to a 180 degree separation in heading. This lines up with the observations one would expect to receive in an urban canyon. The observation elevation angle does not play any role in observability; however, observations with a low elevation angle tend to have more error. When dealing with a filter that only works off two observations, one bad observation can cause a great deal of estimation error.

It is also important to remember that drastic changes in coordinate frame pitch and heading can cause estimation error. Any accurate lane map should not have drastic enough attitude changes to affect the filter.

ACKNOWLEDGMENTS

The Federal Highway Administration is funding this project and others across the range of issues that are critical to the transportation industry through the Exploratory Advanced Research (EAR) Program. For more information, see the EAR Web site at [http://www.fhwa.dot.gov/advancedresearch/about.cfm#focus"](http://www.fhwa.dot.gov/advancedresearch/about.cfm#focus)

REFERENCES

[1] J. Allen, J. Britt, C. Rose, D. Bevly, "Intelligent Multi-Sensor Measurements to Enhance Vehicle Navigation and Safety Systems," presented at the 2009 International Technical Meeting, Anaheim, California, 2009.

[2] J. Britt, D. Bevly, "Lane Tracking using Multilayer Laser Scanner to Enhance Vehicle Navigation and Safety Systems," presented at the 2009 International Technical Meeting, Anaheim, California, 2009.

[3] W. Brogan. *Modern Control Theory*. Upper Saddle River, New Jersey: Prentice Hall, 1991.

[4] J. Clanton, "GPS and Inertial Sensor Enhancement for Vision-Based Highway Lane Tracking," M.S. thesis, Auburn University, Auburn, Alabama, US, 2006

[5] B. Clark, D. Bevly, "GPS/INS Integration with Fault Detection and Exclusion in Shadowed Environments," presented at the 2008 Position Location and Navigation Symposium, Monterey, California, 2008.

[6] J. Farell. *Aided Navigation GPS with High Rate Sensors*. New York, New York: McGraw Hill, 2008.

[7] P. Hughes. *Spacecraft Attitude Dynamics.* Mineola, New York: Dover Publications, 2004.

[8] R. E. Kalman, "A New Approach to Linear Filtering and Prediction Problems," *Trans. Of the ASME-Journal of Basic Engineering*, 82 (Series D), pp. 35-45, 1960.

[9] C. Rose, D. Bevly, "Vehicle Lane Position Estimation with Camera Vision using Bounded Polynomial Interpolated Lines," presented at the 2009 International Technical Meeting, Anaheim, California, 2009.